Constraining Curvature Density Parameter with Strong Gravitational Lenses and Complementary Probes: a Forecast for Next-Generation Surveys

Yang Hu,[1]★ Suhail Dhawan,[2]†

[1]*Mathematical Institute, University of Oxford, Woodstock Road, Oxford OX2 6GG, UK*

[2]*Kavli Institute for Cosmology and Institute of Astronomy, University of Cambridge, Madingley Road, Cambridge CB3 0HA, UK*

9 October 2023

ABSTRACT

Inferring spatial curvature of the Universe with high-fidelity has always been a longstanding and crucial goal in cosmology. With the imminent commissioning of Stage IV surveys, we investigate the constraints on the curvature density parameter, Ω_K, using simulated data from Stage IV strong gravitational lenses (Lens) surveys. We also combine this data with simulated Stage IV type Ia supernovae (SNe Ia) and baryon acoustic oscillations (BAO) data to constrain Ω_K. We present both a parametric approach, assuming either an $o\Lambda$CDM or an owCDM Universe, and a non-parametric approach using Gaussian Process (GP) regression to interpolate the expansion rate $H(z)$, to constrain spatial curvature. Our findings suggest that using Lens data alone, both approaches yield a constraint at the $\sim O(10^{-1})$ level for Stage IV surveys. When combining Lens with SNe Ia and BAO data, the constraint improves to an $\sim O(10^{-2})$ level. Notably, the inclusion of Lens data in the owCDM model breaks the w-Ω_K degeneracy seen in SNe Ia and BAO data, leading to a tighter constraint on spatial curvature comparable to the *Planck* Primary CMB data. This reveals the promise of Stage IV Lens surveys in helping to achieve high-fidelity constraint on Ω_K that is independent of the early-Universe CMB measurement.

Key words: cosmological parameters – cosmology:observations – gravitational lensing:strong

1 INTRODUCTION

The curvature density parameter Ω_K plays a pivotal role in determining the geometric properties of the Universe, and constraining it with high-fidelity has been a longstanding and crucial interest in cosmology. A well-known endeavour to measure spatial curvature is the *Planck* mission through cosmic microwave background (CMB) radiation data. The *Planck* 2015 result indicated a constraint of $|\Omega_K| < 0.005$ (Planck Collaboration et al. (2016)), providing evidence for a spatially flat Universe. Although constraining Ω_K with primary CMB data along encounters limitations due to geometric degeneracy (see e.g., Bond et al. (1997), Efstathiou & Bond (1999), Seljak & Zaldarriaga (1997)), this degeneracy can be effectively broken by incorporating complementary measurements. For instance, the *Planck* 2018 result demonstrated that joint constraints on Ω_K with baryon acoustic oscillation (BAO) measurements (Planck Collaboration et al. (2020)) favored a spatially flat universe to within $\approx 1\sigma$. However, recent studies have raised concerns about the consistency of such combinations, thereby raising the possibility of a "curvature tension" in current data (see e.g. Handley (2021), Valentino et al. (2019, 2021)).

The aforementioned limitations of CMB have sparked interest in using late-Universe probes that are independent of the early-Universe CMB data, such as strong gravitational lenses (Lens), type Ia supernovae (SNe Ia) and BAO, to constrain Ω_K with high-fidelity. Among them, with special attention needed are the studies involving Lens[1]. First suggested by Refsdal (1964), the Lens method involves measuring the time delays between multiple images of a distant source produced by a foreground lensing object. The time delays are related to the time-delay distance $D_{\Delta t}$ to the lens and the source, which has shown sensitivity to the Hubble parameter H_0 and weak dependence on the matter density parameter Ω_m, the dark energy density parameter Ω_Λ, the equation of state parameter of dark energy w, and on Ω_K, at least at face value (see e.g., Linder (2011), Suyu, S. H. & Halkola, A. (2010)).

Despite the seemingly weak dependence of $D_{\Delta t}$ on Ω_K shown

[1] For earlier works, see e.g. Huber, S. et al. (2022), Qi et al. (2022a), Wong et al. (2019) for Lens, Qi et al. (2022b) for strongly lensed type Ia supernovae, Benisty, David & Staicova, Denitsa (2021), Takada & Doré (2015), Yu & Wang (2016) for BAO, Collett et al. (2019), Cao et al. (2021), Denissenya et al. (2018), Li et al. (2019) for combinations of them.

★ E-mail: yang.hu@stcatz.ox.ac.uk (YH)
† E-mail: suhail.dhawan@ast.cam.ac.uk (SD)

in the prior studies, it is essential to acknowledge that past Lens datasets have been limited in both number of Lens events observed and quality of images obtained (see e.g. Wong et al. (2019) on using 6 Lens events). However, the forthcoming era of next-generation surveys, notably exemplified by the Vera C. Rubin Observatory's Legacy Survey of Space and Time (LSST), promises a significant advancement. This survey is anticipated to yield a substantial increase in the count and improvement of the image quality of observed Lens events during its 10-year survey baseline, which includes strongly lensed supernovae and quasars (see e.g. Željko Ivezić et al. (2019), Huber, S. et al. (2019)). Taak & Treu (2023) forecasted that ∼ 1000 strongly lensed quasi-stellar objects will exhibit variability detectable with LSST, while an earlier paper by Oguri & Marshall (2010) claimed that some 3000 strongly lensed quasars and supernovae should have well-measured time-delays. Whether being the more optimistic or realistic case, we aim to investigate whether joint constraints from LSST Lens data and other Stage-IV surveys of complementary late-Universe probes yield consistent results. If this is true, a method worth exploring to achieve high-fidelity constraint on Ω_K is to combine a considerable number of $D_{\Delta t}$ measurements derived from Stage-IV Lens surveys with complementary probes such as SNe Ia and BAO.

In this *Letter*, we use simulated Stage-IV surveys to explore the joint constraint imposed on Ω_K by a large number (∼ 1000–3000) of time-delay distance measurements from Lens and other distance or expansion rate measurements from complementary probes, including SNe Ia and BAO. We present both a parametric and a non-parametric method to do so. In the parametric approach, an *ow*CDM model is adopted to describe the expansion history of the Universe, as this is the simplest model with spatial curvature as a free parameter and also gives freedom to the equation-of-state parameter w for dark energy. In the non-parametric approach, we impose a Gaussian Process (GP) prior on the expansion history, resulting in marginal constraints on Ω_K free from parametric model assumptions. Applying both of our methods to simulated Stage-IV missions data, we forecast that these data will be able to deliver $\sim O(10^{-2})$ level constraints on Ω_K, competitive with the current CMB-only constraints from *Planck* (Planck Collaboration et al. (2020)).

2 METHODOLOGY AND DATA

Strong gravitational lenses (Lens), type Ia supernovae (SNe Ia) and baryon acoustic oscillations (BAO) are all late-Universe distance indicators. In a nutshell, Lens and SNe Ia provide cosmological distance measurements, while BAO give measurements on the expansion rate of the Universe at different redshifts.

2.1 Models

Lens measurements are based on time-delay distances $D_{\Delta t}$, obtained from primary data on time delays and the mass distribution of lensing systems. For the purpose of this *Letter*, we directly employ simulated data at the stage of time-delay distances. Given a Lens system with a foreground lens at redshift z_l and a distant source at redshift z_s ($z_s > z_l$), the associated time-delay distance $D_{\Delta t}$ is given by:

$$D_{\Delta t} = \frac{(1+z_s) D_{A,l} D_{A,s}}{D_{A,ls}}, \tag{1}$$

where $D_{A,l}$ and $D_{A,s}$ are angular diameter distances at lens and source respectively, and $D_{A,ls}$ is the angular diameter distance between lens and source. D_A at a particular redshift z is related to luminosity distance D_L (which SNe Ia is sensitive to) by $D_A = D_L/(1+z)$.

Define $D_h = c/H_0$ and Ω_K the curvature density parameter, $D_{A,ls}$ is given by (cite):

$$D_{A,ls} = \frac{1}{1+z_s}\left(\frac{D_{A,s}}{1+z_s}\sqrt{1+\Omega_K\left(\frac{D_{A,l}}{D_h(1+z_l)}\right)^2} - \frac{D_{A,l}}{1+z_l}\sqrt{1+\Omega_K\left(\frac{D_{A,s}}{D_h(1+z_s)}\right)^2}\right). \tag{2}$$

Note that the dependence of time-delay distance on spatial curvature does not only enter explicitly in Eq. (2), but all the angular diameter distances and luminosity distances depends on Ω_K and other cosmological parameters.

Complementing Lens, SNe Ia provide measurements of the luminosity distance D_L through the distance modulus μ:

$$\mu = 5\lg(D_L) + 25 + M, \tag{3}$$

where M is the absolute SNe Ia calibration (also called absolute magnitude). D_L at redshift z is given by:

$$D_L = \frac{c(1+z)}{H_0\sqrt{|\Omega_K|}}\mathrm{sinn}\left(\sqrt{|\Omega_K|}\int_0^z \frac{dz'}{E(z')}\right), \tag{4}$$

where sinn is sin for $\Omega_K \leq 0$ and sinh for $\Omega_K > 0$. c is the speed of light in vacuum. $E(z) = H(z)/H_0$ is the normalised Hubble parameter (or normalised expansion rate). $H(z)$ can be direclty measured by BAO.

BAO are excellent tracers of the expansion rate of the Universe as a function of redshift, and has been extensively used to infer xxx (cite). Here, $H(z)$ is where parametricity of approaches comes in. In the parametric approach in this *Letter*, we adopt an *ow*CDM model of the Universe, , with o allowing for non-flat geometry and w being the equation-of-state parameter for dark energy[2]. The Hubble parameter $H(z)$ takes the following form:

$$H(z) = H_0\sqrt{\Omega_m(1+z)^3 + \Omega_K(1+z)^2 + \Omega_{DE}(1+z)^{3(1+w)}}, \tag{5}$$

where H_0 is the Hubble's constant, Ω_m is the matter density parameter and Ω_{DE} is the dark energy density parameter, and $\Omega_{DE} = 1 - \Omega_m - \Omega_K$. In this case, the free cosmological parameters are $\boldsymbol{\theta} = (H_0, \Omega_m, \Omega_K, w)$. In the non-parametric approach which we will elaborate in Section 2.3, we do not assume Eq. (5) or any parametric models, and $H(z)$ at arbitrary z is given by Gaussian Process regression on BAO data instead.

2.2 Data and Likelihood

We use the compilation of simulated LSST Lens measurements from LSST Dark Energy Science Collaboration (LSST DESC) et al. (2021). The dataset consists of 310 pairs of simulated lens and source redshifts, denoted as (z_l, z_s). We proliferate the redshift pairs to 1000 and 3000 while maintaining the LSST-like distribution in the original source. However, time-delay distances $D_{\Delta t}$ are not directly provided in this dataset. To address this, we set up a mock universe with specific cosmological parameter values: $\boldsymbol{\theta}_S = (H_0 = 72\ \mathrm{km/s/Mpc}, \Omega m = 0.3, \Omega_K = 0, w = -1)$ and $M = -19.2$ mag. We refer to this mock universe as the *standard setting* Universe in this *Letter*. Using the cosmological parameter values $\boldsymbol{\theta}_S$, we apply Eqs. (1), (2), (4) and (5) to generate mock $D_{\Delta t}$ measurements. Additionally, we generate the corresponding percentage uncertainty σ_{Lens} for each mock $D_{\Delta t}$ measurement, drawn randomly

[2] For an overview of various cosmological models, see e.g. Shi et al. (2012)

from a uniform distribution between 6% to 10%. This range of percentage uncertainties aligns with the expected precision of the LSST survey (Huber, S. et al. (2019)). We collect the generated time-delay distance measurements and uncertainties into a data vector denoted as $\mathbf{d}_{\rm Lens}$. The log-likelihood for Lens data is then given by:

$$\ln P(\mathbf{d}_{\rm Lens}|\boldsymbol{\theta}) = -\frac{1}{2}\sum_i (\hat{D}_{\Delta t,i} - D_{\Delta t,i}(\boldsymbol{\theta}))^2/\sigma^2_{{\rm Lens},i}, \tag{6}$$

where $\hat{D}_{\Delta t}$ is the mock time-delay distance measurement in *standard setting* Universe and $D_{\Delta t}(\boldsymbol{\theta})$ is the time-delay distance at the same redshifts but measured in another Universe with parameter values $\boldsymbol{\theta}$.

For complementary probe SNe Ia, the simulated next-generation survey used in this *Letter* is Nancy Grace Roman Space Telescope (*Roman*), and we use the compilation from Hounsell et al. (2018). The dataset includes redshifts z and a systematics-marginalized covariance matrix $\mathbf{C}_{\rm SN}$ for 40 binned distance moduli measurements. We generate mock distance moduli measurements at the 40 redshifts using Eqs. (3) to (5) in modified *standard setting*[3] and condense it as a data vector $\hat{\boldsymbol{\mu}}$. Together with $\mathbf{C}_{\rm SN}$, they form the data $\mathbf{d}_{\rm SN}$, with log-likelihood given by (up to an additive constant):

$$\ln P(\mathbf{d}_{\rm SN}|\boldsymbol{\theta}, M) = -\frac{1}{2}[\hat{\boldsymbol{\mu}} - \boldsymbol{\mu}(\boldsymbol{\theta}, M)]^T \mathbf{C}^{-1}_{\rm SN}[\hat{\boldsymbol{\mu}} - \boldsymbol{\mu}(\boldsymbol{\theta}, M)], \tag{7}$$

where $\boldsymbol{\mu}(\boldsymbol{\theta}, M)$ represents the distance modulus at the same redshifts in another Universe with parameter values $\boldsymbol{\theta}$ and calibration M.

For the complementary probe BAO, we use simulated data from the Dark Energy Spectroscopic Instrument (DESI) compiled in Dawson et al. (2016). The dataset includes redshifts and percentage uncertainties $\sigma_{\rm BAO}$ in $H(z)$ for 18 measurements. Similar to the previous cases, we generate mock $H(z)$ measurements in the *standard setting* Universe using Eq. (5). We group the mock measurements and uncertainties into a data vector $\mathbf{d}_{\rm BAO}$. In the parametric approach, the log-likelihood for BAO data is given by:

$$\ln P(\mathbf{d}_{\rm BAO}|\boldsymbol{\theta}) = -\frac{1}{2}\sum_i (\hat{H}_i - H_i(\boldsymbol{\theta}))^2/\sigma^2_{{\rm BAO},i}, \tag{8}$$

where $\hat{H}$ is the mock expansion rate measurement in *standard setting* Universe and $H(\boldsymbol{\theta})$ is the expansion rate at the same redshift but measured in another Universe with parameter values $\boldsymbol{\theta}$.

2.3 Prior

In the parametric approach, we impose uniform priors on the cosmological parameters H_0, $\Omega_{\rm m}$, $\Omega_{\rm K}$, w, and the absolute SNe Ia calibration M. The ranges for these priors are shown in Table 1, with the *standard setting* parameter values positioned at about the midpoint of each range. However, the parametric approach has its limitation: the form of the function $H(z)$ in Eq. (5) depends entirely on the choice of parameters. Since $H(z)$ appears everywhere in other relations, all measurable quantities become strongly dependent on the parameters we choose.

To address this limitation and allow for a more flexible representation of $H(z)$, we also introduce a non-parametric approach. Instead of prescribing specific functional forms for $H(z)$, we assume only the general characteristics, such as its smoothness, which are controlled

[3] To account for the variation in the absolute magnitude of each SN Ia event (as known as intrinsic magnitude scattering), we add a small number ϵ randomly drawn from a Gaussian distribution with $\mu = 0$ mag and $\sigma = 0.02$ mag to M so that $M = -19.2 + \epsilon$ mag. This means the calibration for each SN Ia is slightly different but on average $M_{\rm B} = -19.2$.

Table 1. Priors on free cosmological parameters and absolute SNe Ia calibration. The parameter priors with a * are applicable to both the parametric and non-parametric approaches. Those without a * are applicable only to the parametric approach.

Parameter \ Model	owCDM	$o\Lambda$CDM
H_0* [km s^{-1} Mpc^{-1}]	U(0,150)	U(0,150)
$\Omega_{\rm m}$	U(0,0.6)	U(0,0.6)
$\Omega_{\rm K}$*	U(-2,2)	U(-2,2)
w	U(-2,0)	-1
M* [mag]	U(-25,-15)	U(-25,-15)

by a set of hyperparameters denoted as $\boldsymbol{\eta}$. These hyperparameters will be marginalized over during the analysis. To do this systematically, we use Gaussian Process (GP) regression[4] by assigning a GP prior on $H(z)$:

$$P(H(z)|\boldsymbol{\eta}) = \mathcal{N}(H(z)|m(z), k_{\boldsymbol{\eta}}), \tag{9}$$

where $m(z)$ is the prior mean function and $k_{\boldsymbol{\eta}} = k_{\boldsymbol{\eta}}(z_i, z_j)$ is the kernel (or covariance function) that characterises the correlation between measurements of $H(z)$ at different redshifts. The choice of kernel captures the smoothness of the prior function. For this *Letter*, we opt for the squared exponential kernel (or radial basis function), given by:

$$k_{\rm SE}(z_i, z_j) = a^2 \exp\left(\frac{-(z_i - z_j)^2}{2l^2}\right), \tag{10}$$

where hyperparameter a can be interpreted as the characteristic amplitude of $H(z)$, and hyperparameter l represents the characteristic length-scale of redshift z. This kernel is a commonly used choice for modeling smooth functions like $H(z)$.

The non-parametric approach to constraint $\Omega_{\rm K}$ with cosmic chronometers (CCs) data (summarised in Tab. I of Vagnozzi et al. (2021)) and *Pantheon* SNe Ia data has been examine by Dhawan et al. (2021), where a constraint of $\Omega_{\rm K} = -0.03 \pm 0.26$ was obtained. With the data from simulated Stage-IV surveys, we expect to improve this constraint. We partially follow the inference strategy in Dhawan et al. (2021): discretise $H(z)$ into a vector $\mathbf{H}$ at specific redshift nodes z_k. The Gaussian prior on $H(z)$ then becomes a multivariate Gaussian prior on the vector $\mathbf{H}$:

$$P(\mathbf{H}|\boldsymbol{\eta}) = \frac{1}{\sqrt{|2\pi\mathbf{K}_{\boldsymbol{\eta}}|}} \exp\left\{-\frac{1}{2}(\mathbf{H} - \mathbf{m})^T \mathbf{K}_{\boldsymbol{\eta}} (\mathbf{H} - \mathbf{m})\right\}. \tag{11}$$

with mean $\mathbf{m}(z_k) = m(z_k)$ and covariance matrix $\mathbf{K}_{\boldsymbol{\eta},kl} = k_{\boldsymbol{\eta}}(z_k, z_l)$. We ensure that the redshift nodes $\mathbf{H}$ are dense enough to allow for accurate numerical integration of the luminosity distance integrals Eq. (4) involved in the SNe Ia likelihood. The difference between the mentioned work and this *Letter* is that we treat the GP regression step separately from cosmological parameters, and we directly use the predictive mean of $\mathbf{H}$ in Eq. (11) to condition the joint posterior of cosmological parameters. This simplification allows for

[4] A complete guide on GP can be found in Williams (2005).

faster computation and, as we will see in Section 3.2, the uncertainty ignored by doing this on our simulated data is negligible.

To optimise $\boldsymbol{\eta}$, we assume (improper) uniform priors on hyperparameters and sample $\boldsymbol{\eta}$ from the posterior:

$$P(\boldsymbol{\eta}|\mathbf{d}_{\rm BAO}) = P(\boldsymbol{\eta})P(\mathbf{d}_{\rm BAO}|\boldsymbol{\eta}), \tag{12}$$

where $P(\mathbf{d}_{\rm BAO}|\boldsymbol{\eta})$ has a similar form as Eq. (11). After sampling, we take the predictive mean of Eq. (12) as the optimal hyperparameters to be used in Eq. (11).

We use Markov chain Monte Carlo (MCMC) sampling implemented in `emcee` (Foreman-Mackey et al. (2023)) and perform GP in `george` (Foreman-Mackey et al. (2021)). With the non-parametrically interpolated $\mathbf{H}$ obtained from `george`, the remaining free parameters are solely H_0, $\Omega_{\rm K}$, and M.

2.4 Joint Posterior

The treatment of BAO data differs completely between the parametric and non-parametric inference approaches, leading to distinct expressions for the joint posterior. For notatioanl simplicity, we define all the data used in the parametric approach as $\mathbf{d}_{\rm P} = (\mathbf{d}_{\rm Lens}, \mathbf{d}_{\rm SN}, \mathbf{d}_{\rm BAO})$, and define all the data used in the non-parametric approach as $\mathbf{d}_{\rm NP} = (\mathbf{d}_{\rm Lens}, \mathbf{d}_{\rm SN}, \mathbf{H})$.

In the parametric approach, the full joint posterior over $\boldsymbol{\theta} = (H_0, \Omega_{\rm m}, \Omega_{\rm K}, w)$ and M is:

$$\begin{aligned} P(\boldsymbol{\theta}, M|\mathbf{d}_{\rm P}) \propto & P(H_0)P(\Omega_{\rm m})P(\Omega_{\rm K})P(w)P(M) \\ & P(\mathbf{d}_{\rm BAO}|\boldsymbol{\theta})P(\mathbf{d}_{\rm SN}|\boldsymbol{\theta}, M)P(\mathbf{d}_{\rm Lens}|\boldsymbol{\theta}). \end{aligned} \tag{13}$$

In the non-parametric approach, the full joint posterior over H_0, $\Omega_{\rm K}$ and M is:

$$\begin{aligned} P(H_0, \Omega_{\rm K}, M|\mathbf{d}_{\rm NP}) \propto & P(H_0)P(\Omega_{\rm K})P(M)P(\mathbf{H}|H_0, \Omega_{\rm K}, M) \\ & P(\mathbf{d}_{\rm SN}|H_0, \Omega_{\rm K}, M)P(\mathbf{d}_{\rm Lens}|H_0, \Omega_{\rm K}, M). \end{aligned} \tag{14}$$

We sample the joint posterior using MCMC sampling implemented in `emcee`, and marginalise over all other parameters to get the constraint on spatial curvature.

3 RESULT AND ANALYSIS

We show and discuss the result obtained in the parametric and non-parametric approaches using data from simulated Stage-IV surveys of Lens and complementary probes SNe Ia and BAO.

3.1 Result of the Parametric Approach

We apply the parametric approach described above on the simulated datasets $\mathbf{d}_{\rm P}$. Table 2 shows the constraints on all cosmological parameters. Using 1000 Lenses alone, we infer $\Omega_{\rm K} = 0.381^{+0.177}_{-0.321}$ in owCDM model (68% confidence interval). This is a constraint at $\sim O(10^{-1})$. To see the effect of increasing the number of observed Lens events on the constraint, we also divide all percentage uncertainty data in $\mathbf{d}_{\rm Lens}$ by $\sqrt{3000/1000}$ to mimic the case that we observe 3000 Lenses events. With a three-fold increase in number of observed Lens events, we get a less than 50% decrease in the 1σ interval. Based on this, we forecast that Stage-IV LSST Lens data alone is unable to achieve an $O(10^{-2})$ level constraint on $\Omega_{\rm K}$.

The more interesting results are the constraints from the combined data of Lens and SNe Ia. In Table 2, using 1000 Lenses+SNe, we infer $\Omega_{\rm K} = 0.021^{+0.041}_{-0.043}$ in owCDM model. This is a constraint at $\sim O(10^{-2})$, comparable to that of the *Planck* primary data (Planck Collaboration et al. (2020)) and consistent with the forecast in Dhawan et al. (2021). A caveat is that, in the owCDM model, SNe Ia+BAO data also achieve $\sim O(10^{-2})$ constraint, and one can argue that the inclusion of Lens has limited value-addedness. This raises inquiry on how exactly Lens data help to constrain $\Omega_{\rm K}$ in the parametric approach.

To answer this inquiry, we plot w-$\Omega_{\rm K}$ contours in Fig. 1 for single-probe data and combined data in owCDM model, and we also plot a corner plot that shows the constraints on all parameters achieved by Lens alone in Fig. 2. In Fig. 2, the Lens data are shown to be weakly sensitive to both $\Omega_{\rm K}$ and w and strongly sensitive to H_0, consistent with the result in Wong et al. (2019). This demonstrates the existence of w-$\Omega_{\rm K}$ degeneracy in Lens data, which is also present in SNe Ia and BAO data, as seen in the contour plot in Fig. 1. However, the direction of the degeneracy of Lens is different from that of the other two probes. Both SNe Ia and BAO data exhibit an upper-left to bottom-right banana shape, while that of the Lens adopts a bottom-left to upper-right banana shape. This orthogonality is the reason that adding Lens into the data that includes only SNe Ia or BAO break the w-$\Omega_{\rm K}$ degeneracy, thereby tightening the constraint on both w and $\Omega_{\rm K}$.

The reader may further question: if we only consider combining SNe Ia with only one more probe, does Lens help more than BAO on constraining spatial curvature? Fig. 3 gives a clear comparison. We can see that while the inclusion of both lenses and BAO give significant improvement on constraining $\Omega_{\rm K}$, the count of Lens events used matters. Using SNe+BAO, we infer $\Omega_{\rm K} = 0.004^{+0.037}_{-0.098}$, which is a constraint better than 1000Lenses+SNe (number consistent with Taak & Treu (2023)). However, using 3000Lenses+SNe (number consistent with Oguri & Marshall (2010)), we infer $\Omega_{\rm K} = 0.013^{+0.029}_{-0.028}$, which is a constraint better than SNe+BAO in either directions. We can even combine all three probes and infer $\Omega_{\rm K} = -0.016^{+0.015}_{-0.015}$ (with 1000 Lenses) or $\Omega_{\rm K} = -0.014^{+0.014}_{-0.014}$ (with 3000 Lenses).

Under the assumption of the Lens event count and precision used in this *Letter*, we forecast that data from Stage IV Lens surveys are able to break w-$\Omega_{\rm K}$ degeneracy in SNe Ia and BAO data if we assume an owCDM model of the Universe, thereby achieving an $O(10^{-2})$ level constraint on $\Omega_{\rm K}$.

3.2 Result of the Non-Parametric Approach

We apply the non-parametric approach by first GP-fitting $\mathbf{H}$ from $\mathbf{d}_{\rm BAO}$. Given $\mathbf{d}_{\rm BAO}$, we find the optimal hyperparameters for $k_{\rm SE}$ to be $(\alpha, l) = (10.163, 1.924)$. Fig. 4 shows the GP-fitted $\mathbf{H}$. Given the level of precision of $\mathbf{d}_{\rm BAO}$, the width of the 2σ interval is negligible compared to the scale. Hence, instead of treating $\mathbf{H}$ as a distribution, we directly use the predictive mean of $\mathbf{H}$ for the inference of cosmological parameters.

With our non-parametric inference on $\mathbf{H}$, we sample the remaining cosmological parameters by applying the non-parametric approach on $\mathbf{d}_{\rm NP}$. Table 3 shows the result. Using 1000 Lenses along, we infer $\Omega_{\rm K} = 0.014^{+0.042}_{-0.043}$. Using 1000 Lenses+SNe, we infer $\Omega_{\rm K} = -0.009^{+0.014}_{-0.013}$. This is consistent with the two constraints obtained in the parametric approach: the Lens data alone achieve $\sim O(10^{-1})$–$O(10^{-2})$ level constraint, while the combined data with complementary probes achieve $\sim O(10^{-2})$ level constraint. Simulated *Roman* SNe Ia data exhibit the well-known distance-modulus degeneracy, and this degeneracy can be broken by including 1000 simulated LSST Lens data which give $\sim O(10^{-1})$-$O(10^{0})$ level constraint on H_0. On the other hand, adding time-delay distance measurement on SNe Ia data to tighten the constraint on $\Omega_{\rm K}$ give

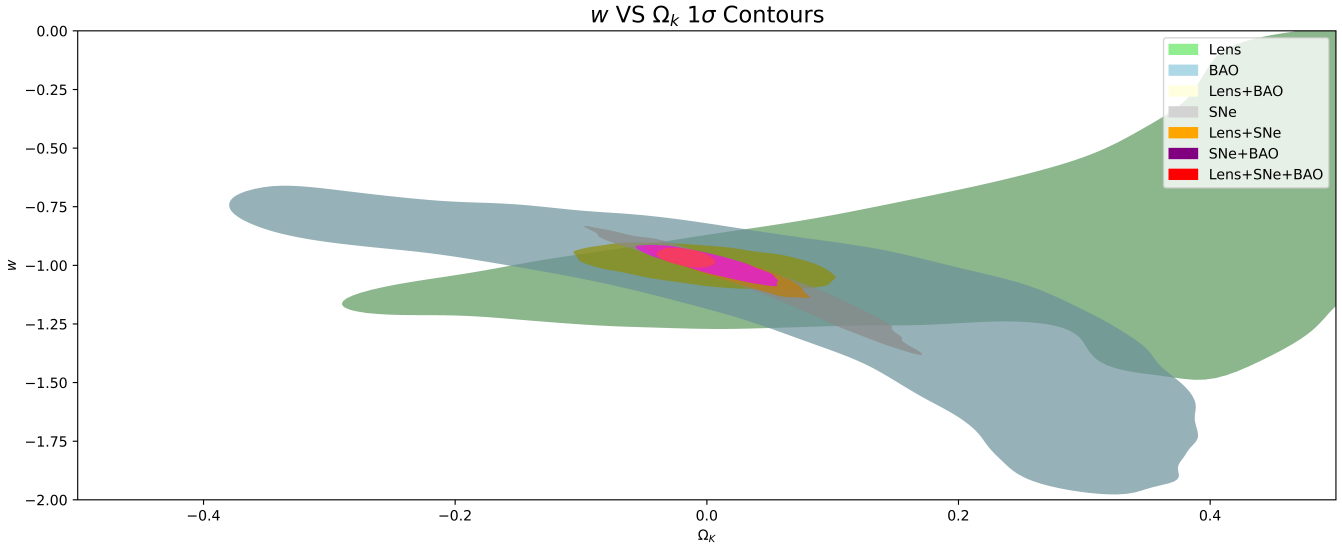

Figure 1. w-Ω_k contours for single-probe and combined data. The number of Lens involved is 1000. The filled regions indicate 1σ intervals.

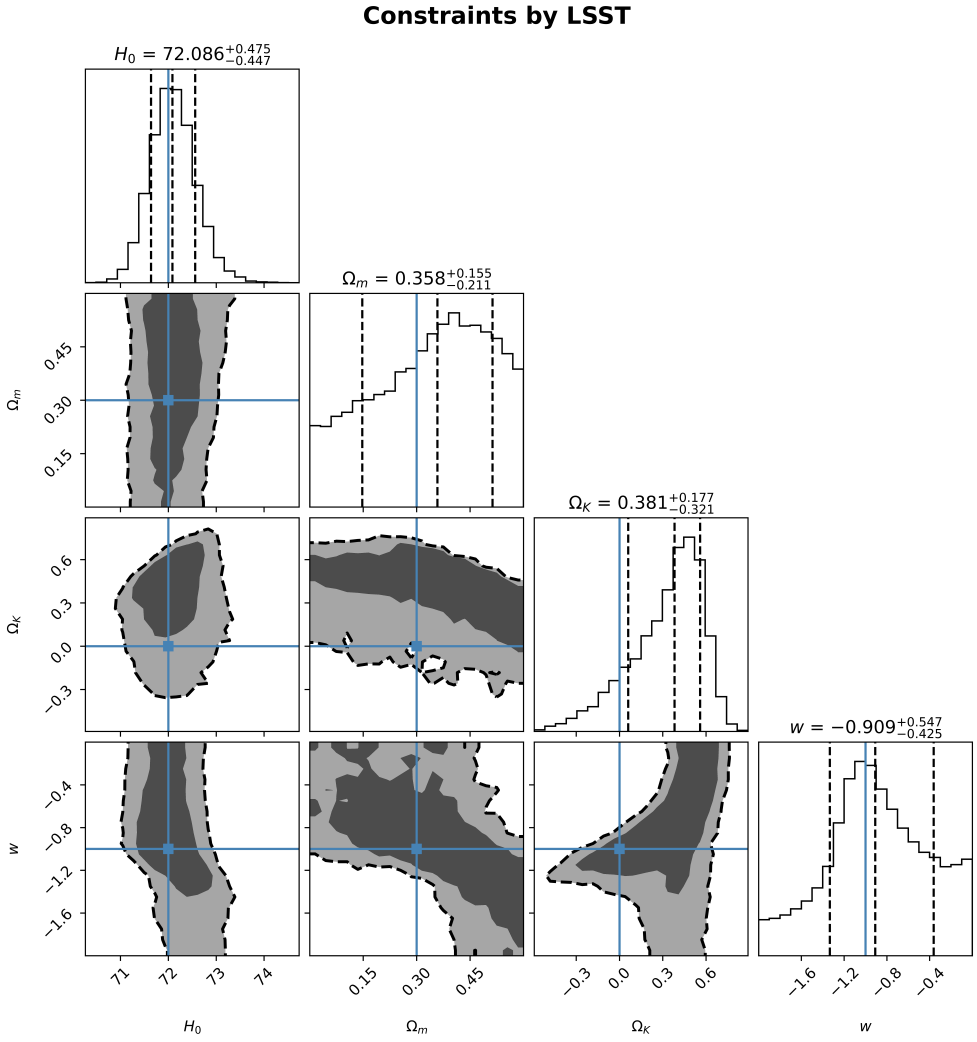

Figure 2. Constraints on various parameters by LSST alone. The number of Lens involved is 1000. The blue lines indicate mock values. The filled black regions indicate 1σ intervals and the light grey regions indicate 2σ intervals.

Table 2. Constraint (68% confidence interval) on various cosmological parameters assuming a parametric form of the expansion rate, using different combinations of simulated Stage-IV surveys of late-Universe probes and different numbers of Lens events.

Model	Probe	H_0 [km s^{-1} Mpc^{-1}]	$\Omega_{\rm m}$	$\Omega_{\rm K}$	w	M [mag]	Equivalent No. of Lens
owCDM	SNe	$74.632^{+21.938}_{-15.093}$	$0.313^{+0.009}_{-0.018}$	$0.051^{+0.075}_{-0.098}$	$-1.080^{+0.165}_{-0.176}$	$-19.117^{+0.560}_{-0.491}$	-
owCDM	SNe+BAO	$71.232^{+0.817}_{-0.825}$	$0.306^{+0.007}_{-0.008}$	$0.004^{+0.038}_{-0.035}$	$-1.080^{+0.165}_{-0.176}$	$-19.117^{+0.560}_{-0.491}$	-
owCDM	Lens	$72.086^{+0.475}_{-0.447}$	$0.358^{+0.155}_{-0.211}$	$0.381^{+0.177}_{-0.321}$	$-0.909^{+0.547}_{-0.425}$	-	1000
owCDM	Lens+SNe	$72.149^{+0.426}_{-0.434}$	$0.310^{+0.008}_{-0.009}$	$0.021^{+0.041}_{-0.043}$	$-1.025^{+0.069}_{-0.078}$	$-19.187^{+0.012}_{-0.012}$	1000
owCDM	Lens+BAO	$72.015^{+0.433}_{-0.426}$	$0.298^{+0.026}_{-0.026}$	$0.002^{+0.067}_{-0.067}$	$-1.002^{+0.063}_{-0.066}$	-	1000
owCDM	Lens+SNe+BAO	$71.788^{+0.193}_{-0.191}$	$0.303^{+0.006}_{-0.006}$	$-0.016^{+0.015}_{-0.015}$	$-0.967^{+0.026}_{-0.027}$	$-19.198^{+0.005}_{-0.005}$	1000
owCDM	Lens	$72.065^{+0.320}_{-0.277}$	$0.361^{+0.143}_{-0.210}$	$0.375^{+0.168}_{-0.330}$	$-0.912^{+0.543}_{-0.368}$	-	3000
owCDM	Lens+SNe	$72.071^{+0.263}_{-0.259}$	$0.308^{+0.007}_{-0.007}$	$0.013^{+0.029}_{-0.028}$	$-1.010^{+0.042}_{-0.046}$	$-19.189^{+0.009}_{-0.009}$	3000
owCDM	Lens+BAO	$72.003^{+0.252}_{-0.248}$	$0.298^{+0.022}_{-0.023}$	$0.002^{+0.050}_{-0.050}$	$-0.999^{+0.043}_{-0.043}$	-	3000
owCDM	Lens+SNe+BAO	$71.840^{+0.151}_{-0.150}$	$0.303^{+0.006}_{-0.006}$	$-0.014^{+0.014}_{-0.014}$	$-0.975^{+0.024}_{-0.025}$	$-19.198^{+0.004}_{-0.004}$	3000

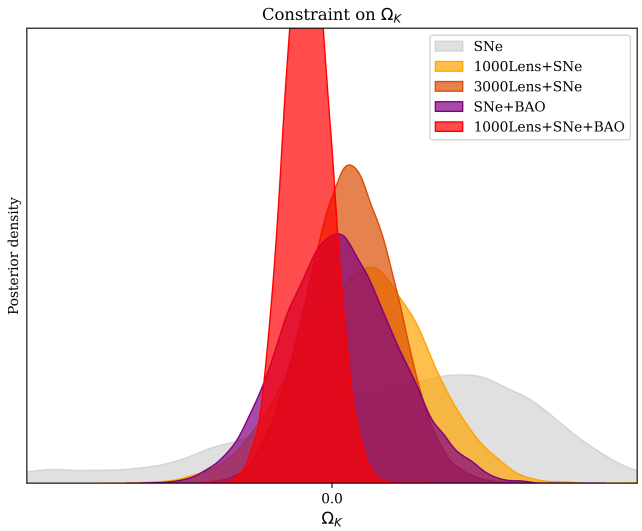

Figure 3. Kernel density estimation for $\Omega_{\rm K}$ for single-probe and combined data, assuming owCDM model of the Universe, from which we infer $\Omega_{\rm K} = 0.021^{+0.041}_{-0.043}$ for 1000Lenses+SNe, $\Omega_{\rm K} = 0.004^{+0.038}_{-0.035}$ for SNe+BAO and $\Omega_{\rm K} = 0.013^{+0.029}_{-0.028}$ for 3000Lenses+SNe (68% confidence interval).

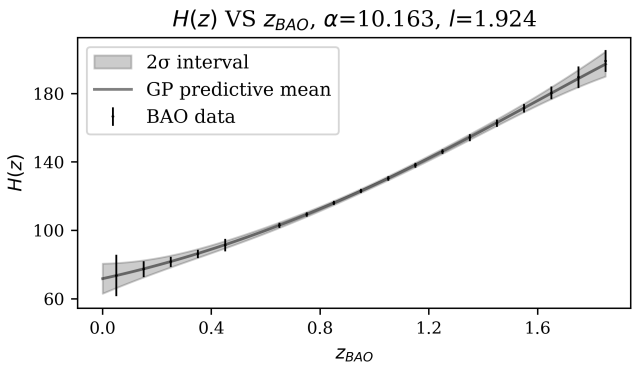

Figure 4. Non-parametric interpolation of **H** with optimal hyperparameters. The solid line is the predictive mean and the grey zone indicates 2σ interval. The kernel used is squared exponential kernel. The hyperparameter amplitude is 10.163 and the hyperparameter length-scale is 1.924.

little value-addedness, as simulated *Roman* data already achieved $\sim O(10^{-1})$ by themselves. Based on this result and using a non-parametric approach with GP-fitted expansion rate, we forecast that data from Stage IV Lens surveys only complement SNe Ia surveys by breaking the distance-modulus degeneracy and tightening the constraint on Hubble's constant H_0, while the Lens data themselves achieve $O(10^{-1})$ level constraint on $\Omega_{\rm K}$ which help little in tightening the constraint on spatial curvature.

4 CONCLUSION

In this *Letter*, we explored the ability of strong gravitational lenses to constrain spatial curvature. Specifically, we took simulated simulated Stage IV Lens survey LSST and 2 complementary probes SNe Ia and BAO to constrain $\Omega_{\rm K}$. Using a parametric approach with an assumed owCDM model of the Universe, we forecast that Lens data alone will reach an $\sim O(10^{-1})$ level constraint on $\Omega_{\rm K}$, and combining Lens data with SNe Ia and BAO data lead to an $\sim O(10^{-2})$ level constraint on $\Omega_{\rm K}$. In this approach, the inclusion of Lens data is crucial in breaking the w-$\Omega_{\rm K}$ degeneracy in SNe Ia and BAO data, thereby achieve a precision comparable to the current *Planck* primary CMB constraints. We also proposed a non-parametric approach to infer spatial curvature, where we GP-fitted the expansion rate $H(z)$ from simulated Stage IV BAO data without assuming any of its parametric form. Based on this interpolated expansion rate, we forecast that Lens data alone will also lead to an $\sim O(10^{-1})$ level constraint on $\Omega_{\rm K}$. However, combining Lens data with SNe Ia data helps little in

Table 3. Constraint (68% confidence interval) on various cosmological parameters with GP-fitted expansion rate, using different combinations of simulated Stage IV surveys of late-Universe probes and different numbers of Lens events.

Probe	Ω_K	Equivalent No. of Lens
Lens	$0.014^{+0.042}_{-0.043}$	1000
SNe	$-0.010^{+0.015}_{-0.015}$	-
Lens+SNe	$-0.009^{+0.014}_{-0.013}$	1000

tightening the constraint on Ω_K, where SNe Ia data alone have already reached $\sim O(10^{-2})$ level constraint. In this approach, Lens data primarily help to constrain cosmological parameter H_0 by breaking the distance modulus degeneracy in SNe Ia data.

Our work is also the first to notice that Lens data with Stage IV survey level's event count and precision have the potential to break the w-Ω_K degeneracy in SNe Ia and BAO data. By using late-Universe probes alone, our inference on spatial curvature is also completely independent of the early-Universe CMB measurements. With an order of $O(10^{-2})$ level constraint achieved on Ω_K and competitive constraints achieved on other cosmological parameters, our work reveals the promise of Stage IV survey of strong gravitational lenses in inference of spatial curvature and other important cosmological parameters.

ACKNOWLEDGEMENTS

Y. H. conducted this research during the Summer Research Internship organised by the Institute of Astronomy, University of Cambridge, where S.D. from Kavli Institute for Cosmology and Institute of Astronomy, University of Cambridge, supervised his project and offered invaluable help and insight throughout the internship.

DATA AVAILABILITY

The data underlying this article will be shared to the corresponding author(s). The associated repository is: https://github.com/YangHu99/CurvatureConstraint

REFERENCES

Benisty, David Staicova, Denitsa 2021, A&A, 647, A38
Bond J. R., Efstathiou G., Tegmark M., 1997, MNRAS, 291, L33
Cao S., Ryan J., Ratra B., 2021, Monthly Notices of the Royal Astronomical Society, 504, 300
Collett T., Montanari F., Räsänen S., 2019, Phys. Rev. Lett., 123, 231101
Dawson K. S., et al., 2016, The Astronomical Journal, 151, 44
Denissenya M., Linder E. V., Shafieloo A., 2018, Journal of Cosmology and Astroparticle Physics, 2018, 041
Dhawan S., Alsing J., Vagnozzi S., 2021, Monthly Notices of the Royal Astronomical Society: Letters, 506, L1
Efstathiou G., Bond J. R., 1999, Monthly Notices of the Royal Astronomical Society, 304, 75
Foreman-Mackey D., Bernhard J., Walker S., Hoyer S., Kamuish Angus R., Mykytyn D., 2021, dfm/george: george v0.4.0, doi:10.5281/zenodo.4541632, https://doi.org/10.5281/zenodo.4541632
Foreman-Mackey D., et al., 2023, dfm/emcee: emcee v3.1.4rc1, doi:10.5281/zenodo.7574785, https://doi.org/10.5281/zenodo.7574785
Handley W., 2021, Phys. Rev. D, 103, L041301
Hounsell R., et al., 2018, ApJ, 867, 23
Huber, S. et al., 2019, A&A, 631, A161
Huber, S. et al., 2022, A&A, 658, A157
LSST Dark Energy Science Collaboration (LSST DESC) et al., 2021, ApJS, 253, 31
Li E.-K., Du M., Xu L., 2019, Monthly Notices of the Royal Astronomical Society, 491, 4960
Linder E. V., 2011, Phys. Rev. D, 84, 123529
Oguri M., Marshall P. J., 2010, Monthly Notices of the Royal Astronomical Society, 405, 2579
Planck Collaboration et al., 2016, A&A, 594, A16
Planck Collaboration et al., 2020, A&A, 641, A6
Qi J.-Z., Hu W.-H., Cui Y., Zhang J.-F., Zhang X., 2022a, Universe, 8, 254
Qi J.-Z., Cui Y., Hu W.-H., Zhang J.-F., Cui J.-L., Zhang X., 2022b, Phys. Rev. D, 106, 023520
Refsdal S., 1964, MNRAS, 128, 295
Seljak U. b. u., Zaldarriaga M., 1997, Phys. Rev. Lett., 78, 2054
Shi K., Huang Y. F., Lu T., 2012, Monthly Notices of the Royal Astronomical Society, 426, 2452
Suyu, S. H. Halkola, A. 2010, A&A, 524, A94
Taak Y. C., Treu T., 2023, Monthly Notices of the Royal Astronomical Society, 524, 5446
Takada M., Doré O., 2015, Phys. Rev. D, 92, 123518
Vagnozzi S., Loeb A., Moresco M., 2021, The Astrophysical Journal, 908, 84
Valentino E. D., Melchiorri A., Silk J., 2019, Nature Astronomy, 4, 196
Valentino E. D., Melchiorri A., Silk J., 2021, The Astrophysical Journal Letters, 908, L9
Williams C. E. R. . C. K. I., 2005, Gaussian processes for machine learning. MIT Press
Wong K. C., et al., 2019, Monthly Notices of the Royal Astronomical Society, 498, 1420
Yu H., Wang F. Y., 2016, The Astrophysical Journal, 828, 85
Željko Ivezić et al., 2019, The Astrophysical Journal, 873, 111

This paper has been typeset from a TEX/LATEX file prepared by the author.